periodica polytechnica

Civil Engineering
56/2 (2012) 245–252
doi: 10.3311/pp.ci.2012-2.11
web: http://www.pp.bme.hu/ci

RESEARCH ARTICLE

Study on collapse behaviors of coarse grained soils

Kuangmin Wei

Received 2011-03-14, revised 2012-02-27, accepted 2012-06-05

Abstract

Collapse deformation of coarse grained materials were studied based on large scale triaxial tests, stress paths of the tests were the same as what soils actually experienced in a rock-fill dam construction, these test results showed that collapse deformation of coarse soils increased with the growth of the stress level sl and the mean stress p, thus, a mathematical model was proposed to relate the collapse deformation to current stress state. The Nanshui model was modified to simulate the post-loading behaviors of the collapsed coarse soils, as was thought important in geotechnical engineering, the modified elastoplastic model conformed with the test data well.

Keywords

Collapse deformation · large scale triaxial tests · collapse model · elastoplastic model

Kuangmin Wei

Institute of Hydraulic Structures, Hohai University, Xikang Road 1, Nanjing 210098

State Key Laboratory of Hydrology, Water Resources and Hydraulic, Engineering, Hohai University, Nanjing 210098, PR China
e-mail: weikuangming2341@163.com

1 Introduction

With the development of roller compacted technology and design technology, coarse soils were widely used in geotechnical engineering(e.g. dam, highway subgrade, airport, etc.). Properties of the coarse soils were researched deeply in the past years. In recent years, many models were developed to predict the mechanical behaviors of the coarse soils(e.g. BBM model, Nanshui model, etc.) [1, 2], but there were still some problems need to be solved, one of which was collapse behavior of coarse soils.

Deformation occur accompanying increases in water content at essentially unchanging the total stresses in partly saturated soils have been originally termed collapse. For low plasticity unsaturated clay, it is accepted that with the increase of the water content results in decrease in matric suction ($u_a - u_w$), thus, wet-induced deformation occurred. But the mechanism of coarse soil's collapse behavior was somewhat different from clay's, It was likely to be caused by breakage and rearrangement of soil particles which were affected by water content(Oldecop & Alonso 2001) [3].

In the twentieth century, coarse soils were more widely used in rock-fill dams, these rock-fill dams have a height of over 200m, some of which even over 300m, and rock-fill dams were becoming the typical structures that filled with coarse soils. Many prototype observation data indicated that collapse deformation occurred at the upstream of the rock-fill dam when the water level rise. This additional deformation may lead to stress redistribution, crack propagation, even a face slab crack in the CFRD(Concrete Face Rock-Fill Dam) when large deformation of rock-fills occur. In the dam construction, a practical method was to increase the initial water content of rock-fill before roller compaction(Fig. 1 & Fig. 2).

It was a long time since the geotechnical engineers focused on collapse behaviors of soils. Nobari & Duncan (1972) [4] conducted triaxial tests with soils in both dry and wet state separately, the strain difference between dry specimen and wet specimen was thought as the collapse strain when they at the same stress state. However, many scholars (Zuo & Zhang et al. 1989, Shen & Yin 2009)[5, 6] thought that stress paths were not consistent with the soils actually experienced in this method, they

suggest a so-called “single triaxial test method”, i.e. in the collapse test, kept the stress state of dry specimen constant, then flooded the specimen, additional deformation during this period was thought to be the collapse deformation. Test results showed that Nobari & Duncan’s method underestimated the collapse deformation. As a result, this paper also adopted “single triaxial test method”, test details will be discussed later.

So far, many constitute models were also developed to predict the collapse behaviors of the coarse soils, (Li 1990[7], Oldecop & Alonso 2001). Sheng *et al*(2004)[8] presented a complete formulation of a constitute model deal with irreversible behavior of unsaturated soil under different loading condition and wet/dry state, which was based on original BBM model. Li(1990) indicated that collapse deformation was totally plastic and the plastic strain increment obeyed the associated flow rule, post-loading behaviors of the collapsed soils were just like overconsolidated in its stress history. Oldecop & Alonso (2001) introduced suction *s* into the constitutive model, which was used to describe the macroscopic phenomena of the rock-fill collapse. By taking the results of an oedometer test, the corresponding model was suggested.

In this paper, large-scale triaxial apparatus was used to reduce the scale effect, which was thought to be an important factor in coarse soils’ tests. A collapse model was proposed to predict the collapse deformation of rock-fills. Collapsed soils were like overconsolidated in its post-loading properties, This paper also modified the NanShui model in order to reflect the post-loading behavior of the collapsed soil.

Fig. 1. Sprinkling water before roller compaction

2 Test procedures and stress paths

2.1 Measured stress paths of the rock-fill dam during dam construction

Amount of prototype observation data showed that the principle stress ratio (σ_1/σ_3) keeps almost constant during the period of the rock-fill dam construction, Wang (2010)[9] analyzed the monitoring data of Sanbanxi rock-fill dam during its construction, positions of the stress cells were shown in Fig. 3. There were four groups of stress cells installed at elevation of 346.2m,

Fig. 2. Roller compaction

each group has two stress cells to monitor the vertical stress σ_y and horizontal stress σ_x, respectively. The relationship of $\sigma_y$and σ_x was plotted in Fig. 4.

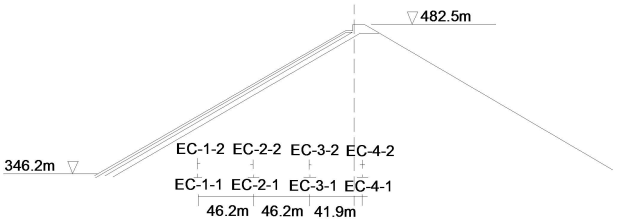

Fig. 3. Position of stress cells in Sanbanxi rock-fill dam

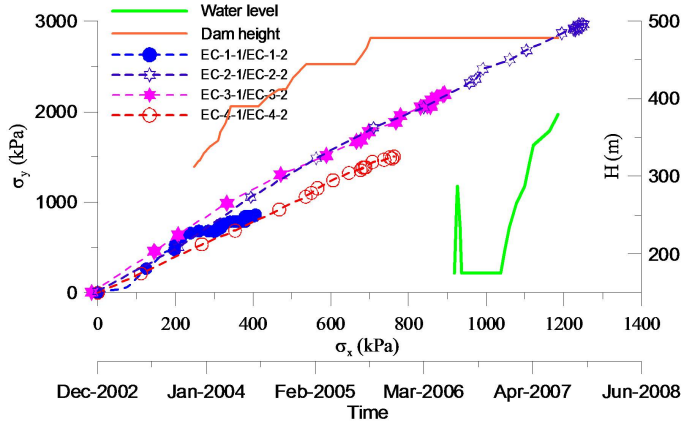

Fig. 4. Relationship of σ_y and σ_x in Sanbanxi rock-fill dam

According to Fig. 4, if the orientation of the first principle stress σ_1 and third principle stress σ_3 were considered to be consistent with σ_y and σ_x, it can be said that, the principle stress ratio (σ_1/σ_3) keeps almost constant during the period of rock-fill dam construction.

In order to simulate the actual stress paths what coarse soils experienced, in the following collapse test, principle stress always kept constant during loading. Principle stress ratio was defined as follows.

$$K_c = \frac{\sigma_1}{\sigma_3} \tag{1}$$

where σ_1 is the first principle stress, σ_3 is the third principle stress.

2.2 Test apparatus and test procedures

This test used *HS1500* large-scale triaxial apparatus (Fig. 5), which was finished in NHRI in 2003, the maximum axial force was 1500KN and the maximum confining pressure could reach 4000 kPa. The axial and lateral loads were all controlled by computer. The parent rock of the test materials were rhyolite, specimens with a sample diameter of 300mm and a height of 700mm, the desired porosity of the sample has a range of 17% to 20%, solid specific gravity was 2.69, the dry density of the sample was 2.15g/mm^3.

Fig. 5. HS1500 triaxial apparatus

The maximum particle size of test soils was controlled less than 60mm. In order to deal with those particles whose sizes were larger than 60mm, this paper used a "similar gradation method" combined with "equivalent substitute method" according to "*Specification of Soil Test(SL 237-1999)*". The gradation of the original rhyolite rock-fill materials as well as the samples were showed in Fig. 6.

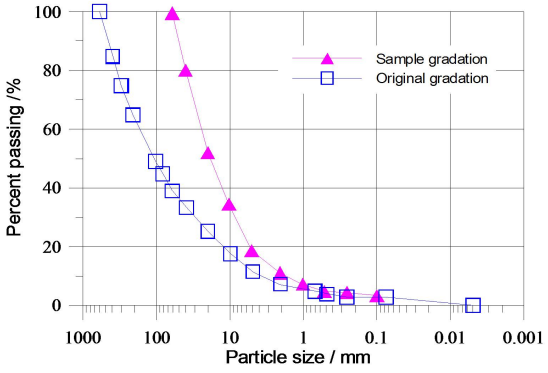

Fig. 6. Gradation of the original rock-fills and samples

At the beginning of the test, rock-fill material was compacted to reach the desired dry density in five sub-layers, then the vertical stress and confining pressure were applied, there were four groups of specimens in this test, their final confining pressures σ_3 were set at 500 kPa, 1200 kPa, 1800 kPa and 2500 kPa respectively. In each group, three specimens experienced different stress paths with their principle stress ratio 1, 2 and 3 respectively.

For each sample, when the confining pressure reached its final value, stopped loading and kept the load constant, waited until the deformation was stable, then turn on the inlet at the bottom of the sample and flooded the whole sample. From then on, collapse deformation occurred, when the deformation of the sample did not increase, measured the additional collapse strain of the sample. After the test, gradations of the samples that experienced different stress paths were measured.

3 Test results and collapse model

3.1 Collapse strain in triaxial tests

Axial strain ε_a and volumetric strain ε_v against the first principle stress σ_1 in four tests were plotted in Fig. 7 to Fig. 10. The horizontal segments of the curves were collapse strain where loads kept constant.

Defined volumetric strain ε_v and general shear strain ε_s as follows

$$\varepsilon_s = \frac{\sqrt{2}}{3}\left[(\varepsilon_1-\varepsilon_2)^2+(\varepsilon_2-\varepsilon_3)^2+(\varepsilon_3-\varepsilon_1)^2\right]^{1/2} \tag{2}$$

$$\varepsilon_v = \varepsilon_1+\varepsilon_2+\varepsilon_3 \tag{3}$$

where ε_i (i=1 to 3) is the principle strain. In the case of axisymmetric, $\varepsilon_2 = \varepsilon_3$, and the general shear strain can be written as

$$\varepsilon_s = \varepsilon_1 - \frac{1}{3}\varepsilon_v \tag{4}$$

From Fig. 7 to Fig. 10, collapse strain of each group was listed in Tab. 1. In Tab. 1, ε_v^s was the collapse volumetric strain, ε_s^s was the general collapse shear strain.

3.2 Particle size distribution change in collapse test

Terzaghi (1960) pointed out breakage of rock particle might lead to rearrangement of the particle structure and a large deformation of rock-fill, however, this effect was enhanced by the presence of water. In this collapse test, particle distribution of each sample was measured in Tab. 2. In Tab. 2, particle group that greater than 20mm showed a deceasing tendency, while particle size smaller than 20mm increased. The breakage of particles increase with both increase of principle stress ratio and confining pressure. Particle size between 0 and 5mm increased most, this implied that breakage of particles usually occur at the local point where particles contact and also a high stress concentration, the present of water could reduce the strength of the contact point, or more easy rearrangement of particle position, therefore, collapse deformation happens, thus, particle breakage may be the fundamental reason for coarse soil's collapse.

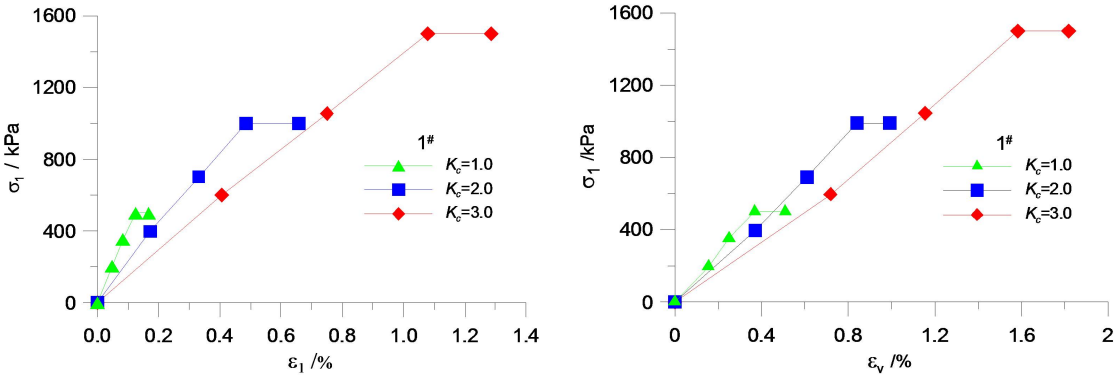

Fig. 7. Collapse test curves with the final confining pressure 0.5 MPa

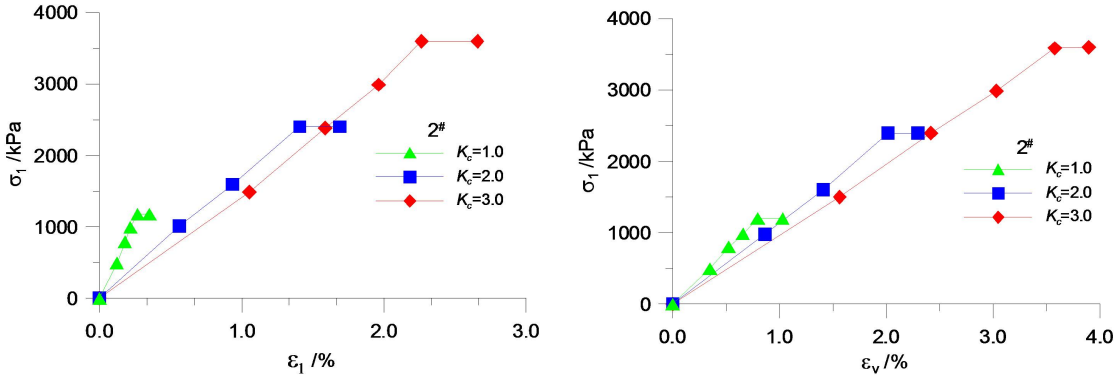

Fig. 8. Collapse test curves with the final confining pressure 1.2 MPa

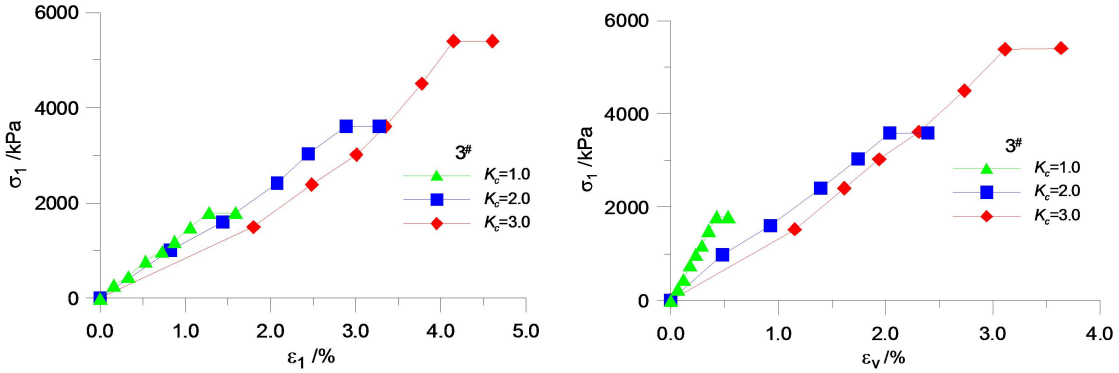

Fig. 9. Collapse test curves with the final confining pressure 1.8 MPa

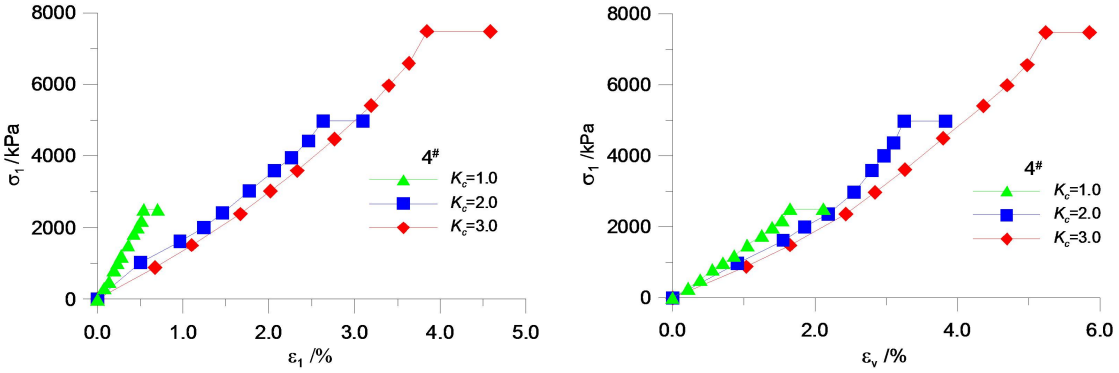

Fig. 10. Collapse test curves with the final confining pressure 2.5 MPa

Tab. 1. Collapse strain of each group in different stress path

Group	1# (σ_3=0.5 MPa)			2 # (σ_3=1.2 MPa)			3 # (σ_3=1.8 MPa)			4# (σ_3=2.5 MPa)		
$K_c = \sigma_1/\sigma_3$	1.0	2.0	3.0	1.0	2.0	3.0	1.0	2.0	3.0	1.0	2.0	3.0
sl	0.000	0.190	0.380	0.000	0.220	0.450	0.000	0.240	0.490	0.000	0.270	0.530
$\Delta\varepsilon_v^s$/%	0.140	0.170	0.200	0.220	0.290	0.320	0.310	0.390	0.440	0.470	0.508	0.620
$\Delta\varepsilon_s^s$ /%	0.000	0.093	0.168	0.000	0.173	0.295	0.000	0.230	0.379	0.000	0.287	0.523

Tab. 2. Gradation change of the coarse soils

Stress state		Percentage content of each particle group /%				
Confining pressure σ_3	K_c	*60~40mm*	*40~20mm*	*20~10mm*	*10~5mm*	*5~0mm*
Original gradation	0.0	20.4	27.9	17.4	15.5	18.4
500 kPa	1.0	19.8	25.9	20.2	15.5	18.6
	2.0	19.2	26.2	19.5	16.0	19.1
	3.0	18.6	26.8	18.7	16.5	19.4
1200 kPa	1.0	19.4	26.2	20.1	15.4	18.9
	2.0	18.9	25.8	19.6	16.2	19.5
	3.0	18.4	26.2	19.1	16.1	20.2
1800 kPa	1.0	19.3	26.1	19.5	15.2	19.9
	2.0	18.6	26.2	18.6	16.3	20.3
	3.0	18.2	25.8	19.2	15.5	21.3
2500 kPa	1.0	19.2	26.0	18.9	15.7	20.2
	2.0	18.3	26.1	18.6	15.6	21.4
	3.0	17.9	25.5	18.6	15.8	22.2

3.3 Collapse model

According to Tab. 1, collapse strain of a specimen was mainly influenced by two factors. For the same confining pressure σ_3 both ε_v^s and ε_s^s increase with the growth of principle stress ratio. The collapse strain also increase with the growth of the confining pressure. In order to describe the volumetric collapse strain and shear collapse of the specimen, here introduced two variables, the mean stress p and stress level *sl*, *sl* was introduced to indicate the degree of shear failure, which is defined by

$$sl = \frac{\sigma_1 - \sigma_3}{(\sigma_1 - \sigma_3)_f} \tag{5}$$

$(\sigma_1 - \sigma_3)_f$ was the shear strength of the specimen in triaxial test. $(\sigma_1 - \sigma_3)_f$ can be expressed according to Mohr-Coulomb criterion

$$(\sigma_1 - \sigma_3)_f = \frac{2C\cos\varphi + 2\sigma_3 \sin\varphi}{1 - \sin\varphi} \tag{6}$$

where C was the cohesion and ϕ as the friction angle, *sl* was used to represent the current stress state, each sample's stress level was listed in Tab. 1. p was given by

$$p = (\sigma_1 + \sigma_2 + \sigma_3)/3 \tag{7}$$

Where σ_i (i=1 to 3) was the principal stress.

Plotted collapse volumetric strain ε_v^s against p/p_a in Fig. 11, and collapse shear strain ε_s^s against $sl * p/p_a$ in Fig. 12, where p_a was the standard atmospheric pressure.

Obviously, collapse volumetric strain can be expressed in exponential form of mean stress p ,collapse shear strain was closely related to both general shear stress q and stress level

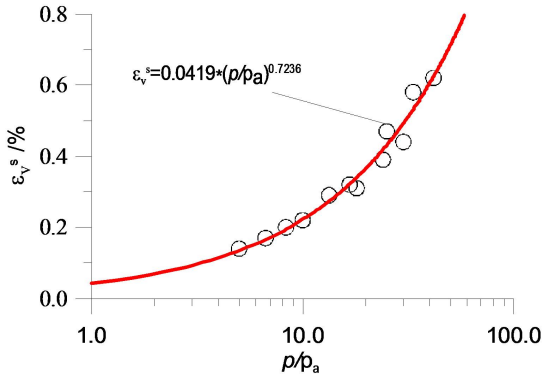

Fig. 11. Relationship between ε_v^s and p/p_a

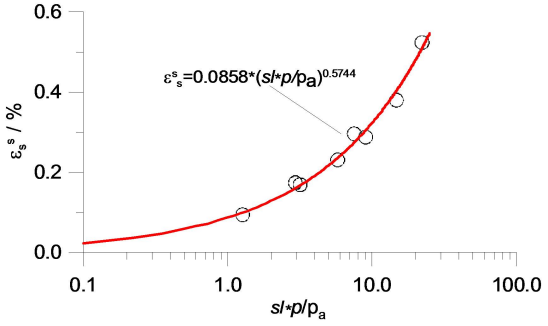

Fig. 12. Relationship between ε_s^s and $sl \cdot p/p_a$

sl,these relations can be described by Eq.(8) and Eq.(9).

$$\Delta\varepsilon_v^s = c_w\left(\frac{p}{p_a}\right)^{n_w} \tag{8}$$

$$\Delta\gamma^s = d_w\left(\frac{p\cdot sl}{p_a}\right)^{m_w} \tag{9}$$

Where c_w, n_w, d_w, m_w were material parameters, which could be specified by fitting the test data in stress and collapse strain figures.

In order to extended the triaxial test results to complex stress state, following the Prandtl-Reuss equation, components of the collapse strain tensor can be expressed as Eq.(10), presuming that orientation of principle stress axes were coincide with principle strain axes (Guo & Li 2002)[10].

$$\begin{Bmatrix}\Delta\varepsilon_x^s\\ \Delta\varepsilon_y^s\\ \Delta\varepsilon_z^s\\ \Delta\varepsilon_{xy}^s\\ \Delta\varepsilon_{yz}^s\\ \Delta\varepsilon_{zx}^s\end{Bmatrix} = \begin{Bmatrix}\frac{\sigma_x-p}{q}\Delta\varepsilon^s\\ \frac{\sigma_y-p}{q}\Delta\varepsilon^s\\ \frac{\sigma_z-p}{q}\Delta\varepsilon^s\\ \frac{\tau_{xy}}{q}\Delta\varepsilon^s\\ \frac{\tau_{yz}}{q}\Delta\varepsilon^s\\ \frac{\tau_{zx}}{q}\Delta\varepsilon^s\end{Bmatrix} + \begin{Bmatrix}\frac{1}{3}\Delta\varepsilon_v^s\\ \frac{1}{3}\Delta\varepsilon_v^s\\ \frac{1}{3}\Delta\varepsilon_v^s\\ 0\\ 0\\ 0\end{Bmatrix} \tag{10}$$

Where q was defined as follows

$$q = \frac{1}{\sqrt{2}}[(\sigma_1-\sigma_2)^2+(\sigma_2-\sigma_3)^2+(\sigma_3-\sigma_1)^2]^{1/2} \tag{11}$$

4 Modified Nanshui model for collapse rock-fill and post-loading behaviors

Collapse model proposed in section 3 could be embed in any constitutive model, decomposing the total strain increments into the sum of three parts

$$\Delta\varepsilon_{ij} = \Delta\varepsilon_{ij}^e + \Delta\varepsilon_{ij}^p + \Delta\varepsilon_{ij}^s \tag{12}$$

where $\Delta\varepsilon_{ij}^e$ was the elastic part of strain increment, $\Delta\varepsilon_{ij}^p$ was the plastic part of strain increment, $\Delta\varepsilon_{ij}^s$ was the collapse strain increment that can be obtained by Eq.(8) to Eq.(10).

The post-loading behavior of collapsed rock-fill was a special phenomenon of coarse soils, because the porosity of the rock-fill decreases without loading in the process of collapse, therefore, the collapsed soils always like in unloading state or overconsolidated state, that means reload the collapsed rock-fill would experience an nearly elastic phase. However, this phenomenon wasn't caused by real stress history. Here, the author used modified Nanshui model to simulate this particular phenomenon of collapsed soils.

4.1 Brief introduction to original Nanshui model

Nanshui model was proposed and developed by Shen (1986; 1994)[11], who used a double-yield -surfaces theory, one surface was so-called "volume yield surface" and the other was so-called "shear yield surface". In Nanshui model, yield surfaces were suggested as follows

$$\begin{cases} f_1 = p^2 + r^2q^2 \\ f_2 = \frac{q^s}{p} \end{cases} \tag{13}$$

where r and s are yield surface parameters to control shape of the surfaces, which usually equal to 2 for rock-fill materials. p and q are defined by Eq.(7) and Eq.(11) respectively.

This model obeyed associated flow rule, stress-strain relationship was expressed as follows

$$\Delta\varepsilon_{ij} = \Delta\varepsilon_{ij}^e + A_1\Delta f_1\frac{\partial f_1}{\partial\sigma_{ij}} + A_2\Delta f_2\frac{\partial f_2}{\partial\sigma_{ij}} \tag{14}$$

where, A_1 and A_2 were positive constant called plastic coefficient,$\Delta\varepsilon_{ij}^e$ the elastic matrix, s_{ij} was the stress tensor. From Eq.(13) and Eq.(14) we get

$$\Delta\varepsilon_v = \frac{\Delta p}{K_e} + \left[4p^2A_1 + \frac{q^{2s}}{p^4}A_2\right]\Delta p + \left[4r^2pqA_1 - \frac{sq^{2s}}{p^3q}A_2\right]\Delta q \tag{15}$$

$$\Delta\varepsilon_s = \frac{\Delta q}{3G_e} + \left[4r^4q^2A_1 + \frac{s^2q^{2s}}{p^2q^2}A_2\right]\Delta q + \left[4r^2pqA_1 - \frac{sq^{2s}}{p^3q}A_2\right]\Delta p \tag{16}$$

In triaxial test, $\Delta p = \frac{\Delta\sigma_1}{3}$, $\Delta q = \Delta\sigma_1$, $\Delta\varepsilon_s = \Delta\varepsilon_1 - \frac{\Delta\varepsilon_v}{3}$, A_1 and A_2 can be expressed as follows by solving the above equations.

$$A_1 = \frac{1}{4q^2}\frac{\eta(\frac{9}{E_t}-\frac{3\mu_t}{E_t}-\frac{3}{G}) + 2s(\frac{3\mu_t}{E_t}-\frac{1}{K_e})}{2(1+3r^2\eta)(s+r^2\eta^2)} \tag{17}$$

$$A_2 = \frac{p^2q^2}{q^{2s}}\frac{(\frac{9}{E_t}-\frac{3\mu_t}{E_t}-\frac{3}{G}) - 2r^2\eta(\frac{3\mu_t}{E_t}-\frac{1}{K_e})}{2(3s-\eta)(s+r^2\eta^2)} \tag{18}$$

In Eq.(17) and Eq.(18) tangent modulus$E_t = \Delta\sigma_1/\Delta\varepsilon_1$ can be determined by Duncan's (Ducan & Chang1970)[12] method as Eq.(19)

$$E_t = k\cdot p_a\left(\frac{\sigma_3}{p_a}\right)^n\left(1 - R_f\frac{(\sigma_1-\sigma_3)(1-\sin\varphi)}{2c\cos\varphi + 2\sigma_3\sin\varphi}\right)^2 \tag{19}$$

In Eq.(19), k, n, R_f were material parameters, p_a was the standard atmospheric pressure, other letters were the same as Eq.(6).

In Eq.(17) and Eq.(18), K_e and G_e were the elastic bulk modulus and the elastic shear modulus, can be converted from

$$\mathrm{K}_e = \frac{E_{ur}}{3(1-2\upsilon)} \tag{20}$$

$$\mathrm{G}_e = \frac{E_{ur}}{2(1+\upsilon)} \tag{21}$$

where E_{ur} was the elastic modulus which can be defined as Eq.(22), υ was the Poisson ratio and was usually set to be a constant value 0.3.

$$E_{ur} = k_{ur}p_a\left(\frac{\sigma_3}{p_a}\right)^{n_{ur}} \tag{22}$$

In Eq.(22) K_{ur} and n_{ur} were material parameters.

In Eq.(17) and Eq.(18) volume ratio $\mu_t = \Delta\varepsilon_v/\Delta\varepsilon_1$ was given by

$$\mu_t = 2c_d\left(\frac{\sigma_3}{p_a}\right)^{n_d}\frac{E_iR_s}{\sigma_1-\sigma_3}\frac{1-R_d}{R_d}\left(1 - \frac{R_s}{1-R_s}\frac{1-R_d}{R_d}\right) \tag{23}$$

$$\eta = \frac{q}{p} \tag{24}$$

where c_d, n_d,R_d were material parameters, $E_i$and R_S were defined by

$$E_i = kp_a\left(\frac{\sigma_3}{p_a}\right)^n \tag{25}$$

$$R_s = R_f \cdot sl \tag{26}$$

where R_f was material parameter, sl was the stress level.

Relationship between stress and strain could be written as follows

$$\Delta p = K_P\Delta\varepsilon_v - P\frac{s_{hk}}{q}\Delta e_{hk} \tag{27}$$

$$\Delta s_{ij} = 2G_e\Delta e_{ij} - P\frac{s_{ij}}{q}\Delta\varepsilon_v - Q\frac{s_{ij}s_{hk}}{q^2}\Delta e_{hk} \tag{28}$$

where $s_{ij} = \sigma_{ij} - p\delta_{ij}$, $e_{ij} = \varepsilon_{ij} - \delta_{ij}(\varepsilon_v/3)$

$$K_p = \frac{K_e}{1 + K_e\alpha}\left(1 + \frac{2GK_e\gamma^2}{1 + K_e\alpha + 2G\delta}\right) \tag{29}$$

$$P = \frac{2G_eK_e\gamma}{1 + K_e\alpha + 2G_e\delta} \tag{30}$$

$$Q = \frac{4G_e^2\delta}{1 + K_e\alpha + 2G_e\delta} \tag{31}$$

$$\alpha = 4p^2A_1 + \frac{q^{2s}}{p^4}A_2 \tag{32}$$

$$\beta = 4q^2r^2A_1 + \frac{q^{2s}s^2}{p^2q^2}A_2 \tag{33}$$

$$\gamma = 4pqr^2A_1 - \frac{q^{2s}s}{p^2q}A_2 \tag{34}$$

$$\delta = \beta + K_e\alpha\beta - K_e\gamma^2 \tag{35}$$

Loading criteria of Nanshui model was as follows: 1 if $f_1 > f_{1max}$ and $f_2 > f_{2max}$ then $A_1 > 0$ and $A_2 > 0$, total loading, A_1 and A_2 can be obtained by Eq.(17) and Eq.(18); 2 if $f_1 \le f_{1max}$ and $f_2 \le f_{2max}$ then $A_1=0$ and $A_2=0$, total unloading; 3 if $f_1 \le f_{1max}$ and $f_2 \ge f_{2max}$ then $A_1=0$ and $A_2 \ge 0$, partially loading, A_2 was calculated by Eq.(18); 4 if $f_1 \ge f_{1max}$ and $f_2 \le f_{2max}$ then $A_1 \ge 0$ and $A_2=0$, partially loading, A_1 was calculated by Eq.(17). Here f_{1max} and f_{2max} represented the maximum stress the soil had experienced in its history.

4.2 Modified Nanshui model for collapsed rock-fill

In Nanshui model, the strain tensor can also be decomposed into the sum of elastic strain, plastic strain and collapse strain like Eq.(12). Collapse tests showed that collapse strain was also unrecoverable. Here, the author introduced “virtual stress” presuming that collapse strain was the plastic strain that caused by virtual force. From the associated flow rule, plastic strain can be expressed as follows

$$\varepsilon_{ij}^p = A_1\Delta f_1\frac{\partial f_1}{\partial\sigma_{ij}} + A_2\Delta f_2\frac{\partial f_2}{\partial\sigma_{ij}} \tag{36}$$

In the Nanshui model f_1 and f_2 were showed in Eq.(13).

Therefore,

$$\Delta\varepsilon_v^p = \left[4p^2A_1 + \frac{q^{2s}}{p^4}A_2\right]\Delta p + \left[4r^2pqA_1 - \frac{sq^{2s}}{p^3q}A_2\right]\Delta q \tag{37}$$

$$\Delta\varepsilon_s^p = \left[4r^4q^2A_1 + \frac{s^2q^{2s}}{p^2q^2}A_2\right]\Delta q + \left[4r^2pqA_1 - \frac{sq^{2s}}{p^3q}A_2\right]\Delta p \tag{38}$$

Assumed that $\Delta\varepsilon_v^s = \Delta\varepsilon_v^p$ and $\Delta\varepsilon_s^s = \Delta\varepsilon_s^p$, make

$$M = 4p^2A_1 + \frac{q^{2s}}{p^4}A_2 \tag{39}$$

$$N = 4r^2pqA_1 - \frac{sq^{2s}}{p^3q}A_2 \tag{40}$$

$$H = 4r^4q^2A_1 + \frac{s^2q^{2s}}{p^2q^2}A_2 \tag{41}$$

Thus virtual force could be deduce from Eq.(37) ~Eq.(41)

$$\Delta p^* = \frac{N\Delta\varepsilon_s^s - H\Delta\varepsilon_v^s}{N^2 - HM} \tag{42}$$

$$\Delta q^* = \frac{M\Delta\varepsilon_s^s - N\Delta\varepsilon_v^p}{MH - N^2} \tag{43}$$

Note that Δp^* and Δq^* were virtual force and they are different from real force, which were used to describe the stress history of rock-fill only, therefore, p and q in Eq.(37) ~Eq.(43) were not directly related to current stress state, because the collapse strain was unlike the plastic strain, collapse strain could occur even below the yield surface, thus here p and $q$were the maximum stress that the soil experienced in its history.

Therefore, f_{1max} and f_{2max} become

$$\begin{cases} f_{1\max} = (p + \Delta p^*)^2 + r^2(q + \Delta q^*)^2 \\ f_{2\max} = \frac{(q+\Delta q^*)^s}{p+\Delta p^*} \end{cases} \tag{44}$$

where p, q were maximum stress that the soil experienced in its history. Δp^* and Δq^* were virtual force used to simulate collapse phenomenon.

4.3 Model predictions

In order to verify the validity of the model, this paper used TSDA program (GU & Zhu 1991)[13] to calculate the stress-strain curves of the collapse rock-fill in the triaxial tests, the test results were also plotted in Fig. 13(a),(b). Test results and model predictions were almost consistent

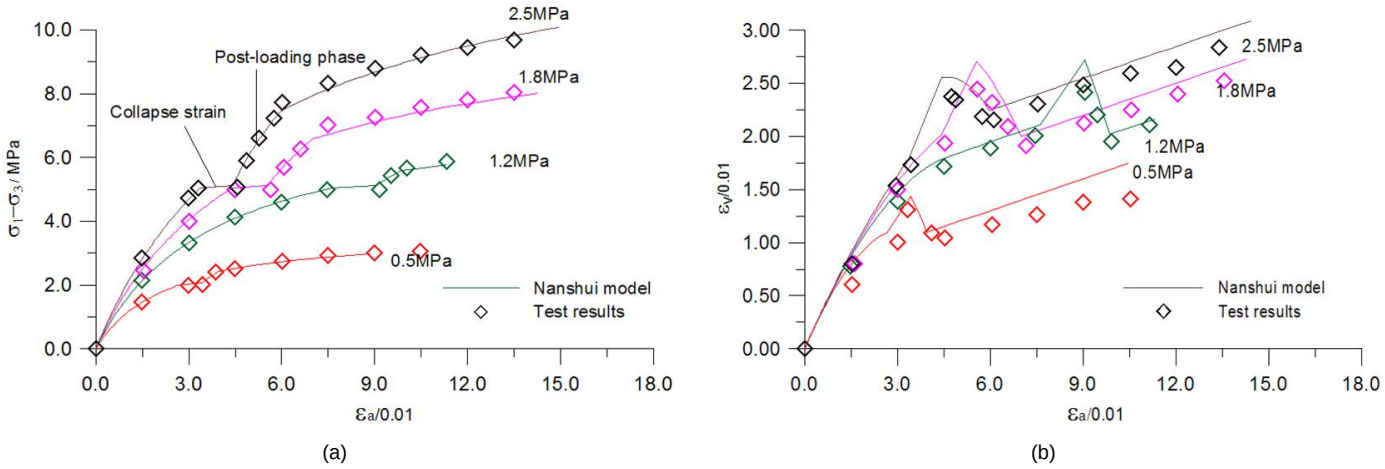

Fig. 13. Comparison of measured and predicted: (a) relationship of $\sigma_1 - \sigma_3$ and ε_a (b) relationship of ε_v and ε_a

5 Conclusions

This paper studied collapse behavior of coarse grained materials based on large triaxial test. Load paths were designed to simulate the actual stress paths of the rock-fill dam. Results showed that shear collapse strain was related to stress level *sl* and the mean stress *p*, volumetric collapse strain was only related to the mean stress *p*. A collapse model was proposed to predict the collapse deformation of the coarse soils. Post-loading behavior was also predicted using modified Nanshui model, the collapsed soils were like overconsolidated to some extent. This model showed a good agreement with test results.

References

1 **Nagy L**, *Permeability of well graded soils*, Periodica Polytechnic Civil Engineering **55** (2011), no. 2, 199–204, DOI Doi: 10.3311/pp.ci.2011-2.12.

2 **Alonso E E, Gens A, Josa A**, *A constitutive model or partially saturated soil*, Geotechnique **40** (1990), no. 3, 405–430.

3 **Jujiang S**, *Nanshui two-yield- surface model and its applications*, Proceedings.of soil mechanics and foundation Engineering Conference (Xi'an,China, October 1994), Proceedings.of soil mechanics and foundation Engineering Conference, China Civil Engineering Society, 2010, pp. 152–159.

4 **Varga G, Czap Z**, *Soil models: safety factors and settlements*, Periodica Polytechnic Civil Engineering **48** (2004), no. 2, 53–63.

5 **Oldecop L A, Alonso E E**, *A model for rockfil compressibility*, Geotechnique **51** (2001), no. 2, 127–139.

6 **Nobari E S, Duncan J M**, *Effect of reservoir filling on stresses and movements in earth and rockfill dams*, Department of Civil Engineering, University of California, 1972.

7 **Yuanming Z, Wenxi Z, Zhujiang S.**, *Study of soaking properties of rockfills in Xiaolangdi dam*, Proceedings of the 1st East Geotechnical Engineering Conference (Nanjing,China, October 1989), Proceedings of the 1st East Geotechnical Engineering Conference, Tongfang HowNet (Beijing) Technology Co., Ltd., 1989, pp. 363–370.

8 **Guangjun S, Zongze Y.**, *Improvment of wetting deformation analysis method of coarse-grained materials*, Chinese Journal of Rock Mechanics and Engineering **28** (2009), no. 12, 2438–2444.

9 **Guangxin L**, *Tests of collapse rock-fills and its mathematic models*, Chinese Journal of Geotechnical Engineering **12** (1990), no. 5, 59–64.

10 **Sheng D, Sloan S., Gens A**, *A constitutive model for unsaturated soils: thermomechanical and computational aspects*, Computational Mechanics **33** (2004), 453–465.

11 **Yongming W**, *Study on the Scale Effect and Elastoplastic Model of Coarse-grained Materials*, PhD thesis, Hohai University, Nanjing, Jiangsu, China, 2010.

12 **Yaoming G, Guoying Li**, *Study of rheology and collapse behaviors of rockfills in CFRD*, Engineering Mechanics **Suppl** (2002), 746–749.

13 **Zhujiang S**, *Elasto-plastic analysis of consolidation and deformation of soft ground*, Scientia Sinica **XXIX** (1986), no. 2, 210–224.

14 **Duncan J M, Chang G Y**, *Non-linear analysis of stresses and strain in soils*, Journal of the Soil Mechanics and Foundations Division **96** (1970), no. 5, 1629–1652.

15 **Ganchen G U, Sheng Z**, *Three-dimensional nonlinear finite element program in static and dynamic analysis of CFRD*, Science & Technology Press, Beijing, 1991.